MgATP and Fructose 6-Phosphate Interactions with Phosphofructokinase from *Escherichia coli*†

Jason L. Johnson and Gregory D. Reinhart*,‡

Department of Chemistry and Biochemistry, University of Oklahoma, Norman, Oklahoma 73019

Received June 24, 1992; Revised Manuscript Received September 9, 1992

ABSTRACT: A thermodynamic linked-function analysis is presented of the interactions of MgATP and fructose 6-phosphate (Fru-6-P) with phosphofructokinase (PFK) from *Escherichia coli* in the absence of allosteric effectors. MgATP and Fru-6-P are shown to bind in random fashion by product inhibition of the back-reaction as well as by the kinetically competent binding of each ligand individually as monitored by the consequent changes in the intrinsic fluorescence of *E. coli* PFK. When Fru-6-P is saturating, the dissociation of MgATP is sufficiently slow that it cannot achieve a binding equilibrium in the steady state, causing the observed K_m (49 μM) to significantly exceed the K_d (1.7 μM) deduced from a thermodynamic linkage analysis. The following features distinguish the interactions of MgATP and Fru-6-P with *E. coli* PFK: MgATP and Fru-6-P antagonize each other's binding to the enzyme in a saturable manner with an overall apparent coupling free energy equal to +2.5 kcal/mol at 25 °C; MgATP induces positive cooperativity in the Fru-6-P binding profile, with the Hill coefficient calculated from the Fru-6-P binding curves reaching a maximum of 3.6 when MgATP is saturating; and MgATP exhibits substrate inhibition at low concentrations of Fru-6-P. Simulations based upon the rate equation pertaining to a two-active-site, two-substrate dimer indicate that these features can all result from two independent couplings: an antagonistic MgATP–Fru-6-P coupling extending at least in part between active sites and a MgATP-induced Fru-6-P–Fru-6-P coupling. The average magnitudes of these couplings are estimated to equal +1.1 and −1.3 kcal/mol at 25 °C, respectively.

Escherichia coli PFK[1] (EC 2.7.1.11) is a tetrameric allosteric enzyme that catalyzes the phosphorylation of Fru-6-P to Fru-1,6-BP, with MgATP serving as the phosphoryl donor. When MgATP is saturating, PFK shows cooperative kinetics with respect to Fru-6-P binding, while saturation profiles are hyperbolic with respect to MgATP at high Fru-6-P concentrations (Blangy et al., 1968). Control of the activity of *E. coli* PFK is thought to derive physiologically from the effectors PEP and ADP. Both the inhibitor PEP and the activator ADP allosterically alter the apparent affinity of the protein for Fru-6-P, while the maximal catalytic activity remains unchanged (Blangy et al., 1968). This allosteric control has been described in terms of the concerted transition theory (Monod et al., 1965; Rubin & Changeux, 1966; Blangy et al., 1968). According to this two-state model, an equilibrium exists between an active "R" conformation having an optimal binding site for substrate and an inactive "T" conformation with very low substrate affinity. Shifts in this equilibrium occur when the allosteric activator and inhibitor bind preferentially to the R and T states, respectively.

A regulatory role for the substrate MgATP has recently been proposed for *E. coli* PFK (Berger & Evans, 1991). It was demonstrated through the steady-state quenching of PFK's intrinsic tryptophan fluorescence that Fru-6-P in the absence of MgATP binds with much greater affinity than at saturating MgATP. A more recent kinetic investigation into this phenomenon has revealed a mutually antagonistic relationship between the two substrates MgATP and Fru-6-P (Deville-Bonne, et al., 1991b) when monitored under saturating GDP concentrations to abolish Fru-6-P cooperativity (Blangy et al., 1968). Deville-Bonne et al. (1991b) concluded that MgATP and Fru-6-P bind in a rapid-equilibrium random manner with mutual antagonism arising when both substrates bind within each single active site.

Berger and Evans (1991) have attempted to explain the actions of MgATP within the context of the R and T model used to explain the effects of the allosteric effectors. From this perspective, since MgATP antagonizes Fru-6-P binding and exhibits substrate inhibition at low Fru-6-P concentrations, it promotes the formation of the inhibited T conformation. When Fru-6-P is bound, subsequent binding of MgATP maintains the R state since MgATP binding is not cooperative. Free enzyme, which binds Fru-6-P with high affinity, is thought to exist in the R form. However, this model fails to explain how MgATP can simultaneously bind to the R form with high affinity and promote the formation of the T form. Berger and Evans (1991) recognized this inconsistency and suggested that MgATP may bind to a second allosteric site, although there is a growing recognition that the R–T model itself is likely insufficient to explain these and other regulatory features of *E. coli* PFK (Kundrot & Evans, 1991; Deville-Bonne et al., 1991a).

In the present work, carried out in the absence of allosteric effectors, steady-state fluorescence, multi-frequency phase fluorometry, and enzyme kinetics are used to quantify the binding of each substrate in the presence and absence of the other. Both the affinity and the apparent cooperativity of the binding profiles are evaluated. Our point of view focuses on the properties of the four enzyme species that can be defined

† Supported by Grants GM 33216 from the National Institutes of Health and HRO-025 from the Oklahoma Center for the Advancement of Science and Technology.

* Author to whom correspondence should be addressed.

‡ Recipient of an Established Investigator Award from the American Heart Association.

[1] Abbreviations: PFK, phosphofructokinase; Fru-6-P, fructose 6-phosphate; Fru-1,6-BP, fructose 1,6-bisphosphate; PEP, phosphoenolpyruvate; BCA, bicinchoninic acid; SDS, sodium dodecyl sulfate; HEPPS, *N*-(2-hydroxyethyl)piperazine-*N*′-3-propanesulfonic acid; MOPS, 3-(*N*-morpholino)propanesulfonic acid.

0006-2960/92/0431-11510$03.00/0

unambiguously: free enzyme with neither MgATP nor Fru-6-P bound, enzyme fully saturated with bound MgATP, enzyme fully saturated with bound Fru-6-P, and enzyme with a catalytically competent ternary complex at each of its four active sites. Product inhibition studies of the back-reaction kinetics provide patterns that confirm that MgATP and Fru-6-P bind to free enzyme in a random sequential mechanism. However, a linked-function analysis of the data reveals that the K_m for MgATP does not provide a reasonable estimate of its thermodynamic dissociation constant when Fru-6-P is saturating. Nonetheless, the coupling free energy between the mutually antagonistic substrates and the apparent homotropic coupling free energy associated with Fru-6-P binding at saturating MgATP can be estimated. The properties of the enzyme, including the cooperativity displayed by Fru-6-P binding at high MgATP concentrations and the substrate inhibition by MgATP at low Fru-6-P concentrations, are shown to be a direct consequence of these two coupling interactions and the oligomeric nature of the enzyme.

MATERIALS AND METHODS

Materials. PFK was purified from *E. coli* K12, carrying the wild-type PFKA gene obtained as a frozen paste from Grain Products Corporation. All chemical reagents used in buffers, PFK purification, and enzymatic assays were of analytical grade, purchased from either Sigma, Fisher, or Aldrich. Matrex Gel Blue A–agarose resin for affinity chromatography was obtained from Amicon Corp. Creatine phosphate, the potassium salts of ADP, and the sodium salts of Fru-6-P, Fru-1,6-BP, ATP, and PEP were obtained from Sigma. The coupling enzymes aldolase, triosephosphate isomerase, glycerol-3-phosphate dehydrogenase, phosphoglucoisomerase, hexokinase, and glucose-6-phosphate dehydrogenase in ammonium sulfate suspensions and creatine kinase in lyophilized form were obtained from Boehringer Mannheim. Coupling enzymes were dialyzed extensively against a buffer consisting of 50 mM MOPS–KOH, 100 mM KCl, 5 mM $MgCl_2$, and 100 μM EDTA at pH 7.0. Deionized distilled water was used throughout.

PFK Purification. PFK was purified via the method of Kotlarz and Buc (1982) with the following modifications. The cell extract, clarified by centrifugation after treatment with deoxyribonuclease I, was loaded at 15 mL/h onto a 15 cm × 0.85 cm Matrex Gel Blue A–agarose affinity column. The column was then rinsed at 15 mL/h in the following three-step series: 300–500 mL of buffer A (Kotlarz & Buc, 1982), buffer A + 1.5 M NaCl until the absorbance at 280 nm of the eluate decreased below 0.05, and buffer A + 2 mM ATP until the absorbance at 595 nm of the eluate fell below 0.03 after reaction with Bio-Rad Bradford protein reagent (Bradford, 1976). Elution of PFK was then accomplished via the application of buffer A + 2 mM ATP + 1.5 M NaCl. Fractions containing the highest specific activity were dialyzed against buffer A + 2 mM ATP and subsequently applied to the Mono Q HR 5/5 anion-exchange column produced by Pharmacia for FPLC. A linear 0–1 M NaCl gradient was used to elute the PFK. Fractions with high specific activity were pooled and dialyzed against a 50 mM HEPPS buffer for storage. A 60% yield and specific activity of 205–220 units/mg were generally obtained, with homogeneity demonstrated by a single band on SDS–polyacrylmide gel electrophoresis.

Enzyme Activity Determination. Activity determinations for the forward reaction were carried out in 1.0 mL of a HEPPS buffer adjusted to pH 8.0 at 25 °C and containing 50 mM HEPPS–KOH, 10 mM $MgCl_2$, 10 mM NH_4Cl, 0.1 mM EDTA, 2 mM dithiothreitol, 0.2 mM NADH, 250 μg of aldolase, 50 μg of glycerol-3-phosphate dehydrogenase, 5 μg of triosephosphate isomerase, and the Fru-6-P and MgATP concentrations indicated in the text. When assays were performed at low MgATP concentrations, 3 mM creatine phosphate and 30 μg/mL creatine kinase served as an ATP-regenerating system. To initiate the enzymatic reaction, 20 μL of PFK, suitably diluted in a buffer containing the coupling enzymes, was added to the mixture. The steady-state reaction rate was determined by monitoring the decrease in absorbance at 340 nm with respect to time, caused by the oxidation of NADH, with a strip-chart recorder. Rates were determined after the completion of any pre-steady-state transients.

The back-reaction, in which Fru-6-P and MgATP are formed from MgADP and Fru-1,6-BP, was assayed with the same buffer as was utilized in the forward reaction assays just described. Two separate coupling enzyme systems were used. To monitor inhibition by MgATP, a 1.0-mL assay mixture contained 16 μg of phosphoglucoisomerase, 4 μg of glucose-6-phosphate dehydrogenase, and 1 mM NADP. For the product inhibition by Fru-6-P, 1.0 mL of the assay mixture contained 16 μg of hexokinase, 4 μg of glucose-6-phosphate dehydrogenase, 10 mM glucose, and 1 mM NADP. In both cases, the reaction rate was followed by measuring the increase in absorbance at 340 nm caused by the reduction of NADP.

Protein Determination. Protein determinations were accomplished using the BCA protein assay reagent (Smith et al., 1985). By ensuring that both standards and unknowns consisted of 10% buffer, potential interferences by buffer reagents were avoided.

Fluorescence Measurements. Steady-state intensity of the intrinsic PFK fluorescence was measured on an ISS Model K2 multifrequency phase fluorometer using a xenon arc lamp as an excitation source. Excitation was performed at 300 nm, and emission was collected through a Schott WG-345 filter for Fru-6-P titration experiments and through a Schott WG-320 filter for MgATP titration experiments. Titration experiments were performed in 50 mM HEPPS–KOH (pH = 8.0), 10 mM $MgCl_2$, 10 mM NH_4Cl, and 0.2 mM EDTA, and all intensity measurements were corrected for any contribution made by this buffer. PFK subunit concentration was equal to 0.8 μM and 0.1 μM for the Fru-6-P and MgATP titration experiments, respectively. The fractional binding saturation by either ligand was calculated from the intensity variation with free ligand concentration by calculating the quantity $|F^0 - F|/|F^0 - F^\infty|$ where F^0 represents the emission intensity in the absence of ligand, F^∞ equals the emission intensity when the ligand is saturating, and F corresponds to the intensity after the addition of a particular concentration of ligand.

Frequency domain fluorometry was performed with an ISS K2 multifrequency phase fluorometer, using the 300-nm line of a Spectra-Physics Model 2045 argon ion laser as an excitation source. The excitation beam was passed through a 2-mm-thick Schott WG-290 filter to remove the 275-nm line which is also produced by this laser when operated in the "deep-UV" mode. Emission was measured through a Schott WG-345 cut-on filter and a Corning 7-54 band-pass filter. Buffer conditions were identical to those described for steady-state fluorescence measurements, while the PFK-subunit concentration was 2.7 μM. Data acquisition was made with ISS software, while analysis was performed with GLOBALS UNLIMITED, obtained from the Laboratory for Fluorescence Dynamics at the University of Illinois at Urbana–Champaign.

Table I: Product Inhibition Patterns for Back-Reaction

[FBP] (mM)	[MgADP] (mM)	inhibitor	pattern[a]	K_{is} (μM)	K_{ii} (μM)
varied	0.06	Fru-6-P	C	17 ± 1	NA[b]
5.0	varied	Fru-6-P	NC	13 ± 1	46 ± 2
varied	0.2	MgATP	NC[c]	20 ± 8	230 ± 9
1.0	varied	MgATP	C[c]	27 ± 1	NA

[a] NC = noncompetitive; C = competitive. [b] Not applicable. [c] Inhibition pattern complicated somewhat by the appearance of cooperativity in the binding of the variable substrate. However, the general features conformed to those expected for the indicated inhibition, and the replots of $1/V_{max}$ and/or $K_{1/2}/V_{max}$ were sufficiently linear so that inhibition constants could be determined in the usual manner. See text for further explanation.

EXPERIMENTAL RESULTS

Back-Reaction. In the back-reaction, Fru-1,6-BP and MgADP bind noncooperatively in the absence of MgATP and Fru-6-P. Initial velocity data for the back-reaction fit well to the following equation which describes either an ordered or rapid-equilibrium-random bi–bi mechanism (Cleland, 1963):

$$v = \frac{V_{max}[A][B]}{K_{ia}K_b + K_b[A] + K_a[B] + [A][B]} \quad (1)$$

where A = Fru-1,6-BP and B = MgADP. The following kinetic parameters were obtained from nonlinear regression analysis, performed as described by Cleland (1967): V_{max} = 39 s^{-1}; K_a = 1.85 ± 0.07 mM; K_{ia} = 2.46 ± 0.22 mM; K_b = 51 ± 2 μM; and $K_{ib} = K_{ia}K_b/K_a$ = 68 ± 5 μM (data not shown).

The results of product inhibition of the back reaction are summarized in Table I. Inhibition by Fru-6-P was easily interpreted as either noncompetitive or competitive inhibition patterns because all experiments produced linear double-reciprocal plots and replots. Inhibition by MgATP often produced substrate binding profiles that exhibited a modest amount of binding cooperativity, with Hill coefficients never exceeding 1.5. When MgADP was the variable substrate, V_{max} was clearly invariant, and the value of $K_{1/2}$ for MgADP increased linearly with MgATP concentration, behavior consistent with a competitive-type inhibition and in agreement with the competitive inhibition observed between MgATP and MgADP for the forward reaction of *E. coli* PFK (Blangy et al., 1968). When Fru-1,6-BP was the variable substrate, both $K_{1/2}/V_{max}$ and $1/V_{max}$ varied in a linear manner as a function of MgATP concentration as expected for noncompetitive inhibition.

Fru-6-P and MgATP Binding to Free Enzyme. The hyperbolic binding of Fru-6-P to *E. coli* PFK in the absence of MgATP can be monitored by the ensuing quenching of the intrinsic PFK fluorescence. A plot of fraction binding saturation as a function of Fru-6-P concentration is presented in Figure 1A. A Hill plot analysis (1910) of these data indicates a K_d equal to 6.8 μM and a Hill coefficient approximately equal to 1. The Fru-6-P binding event was also monitored by a decrease in fluorescence lifetime of the intrinsic fluorescence which accompanies the drop in emission intensity. In the absence of ligands, the fluorescence decay of the four identical tryptophan moieties per tetramer in *E. coli* PFK fits best to two exponentials, with greater than 94% of the emission deriving from a single discrete lifetime of 5.6 ns. The minor component exhibits a lifetime of 0.9 ns. Upon saturation by Fru-6-P, the lifetime of the large component decreases to 4.7 ns. The small lifetime component does not vary with Fru-6-P concentration and therefore was fixed in the analysis. Fitting the data obtained at intermediate concentrations of Fru-6-P to a sum of two exponentials corresponding to the free and Fru-6-P bound lifetimes, respectively, allowed the determination of the relative concentrations of free and bound, from which we determined the binding profile also shown in Figure 1A. The entire data set exhibited a value for the global χ^2 of 1.95. Essentially the same binding curve is described by both the intensity and lifetime data.

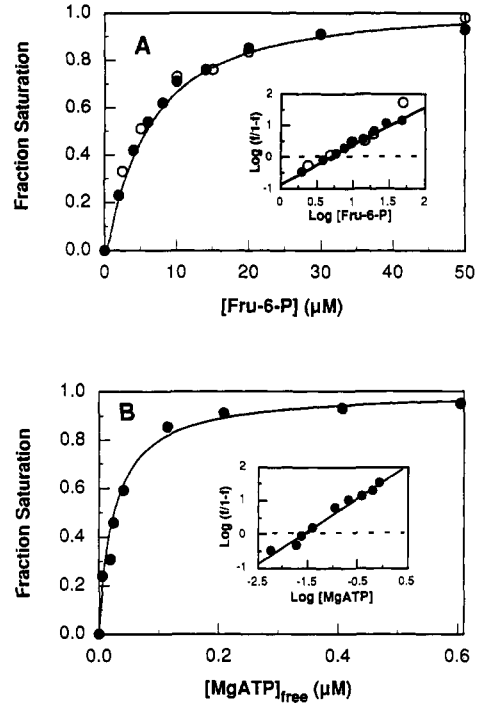

FIGURE 1: (A) Binding of Fru-6-P to *E. coli* PFK as followed by the decrease in intrinsic PFK fluorescence intensity (●) and lifetime (○). Percent saturation was calculated in each case as described in the text. (B) Binding of MgATP to *E. coli* PFK as followed by the concomitant increase in intrinsic PFK fluorescence. Percent saturation and free concentration of MgATP were calculated as described in the text. The inset to each panel shows a corresponding Hill plot of the data.

MgATP also modifies the intrinsic fluorescence of *E. coli* PFK so that binding of MgATP can be observed under equilibrium conditions. Saturation with MgATP causes a 14% increase in emission intensity and roughly a 0.1-ns increase in the fluorescence lifetime, although the latter perturbation was too small to utilize effectively in titration experiments. By considering the fraction of the total increase in fluorescence associated with the titration of a given total MgATP concentration, the concentration of unbound MgATP was calculated. A plot of fraction bound versus free MgATP concentration, and the corresponding Hill plot, is shown in Figure 1B. A K_d of 0.025 μM and a Hill coefficient of 1 were obtained.

Fru-6-P and MgATP Binding with the Other Substrate Saturating. The binding profiles of Fru-6-P and MgATP alone to free enzyme shown in Figure 1 contrast markedly with the apparent binding profiles obtained by following catalytic turnover when the nonvaried substrate is saturating, as shown in Figure 2. In the absence of allosteric effectors and at a saturating concentration of MgATP (3 mM), Fru-6-P appears to bind cooperatively, as shown in Figure 2A. The concentration of Fru-6-P producing half-maximal velocity, $K_1/_2$, is equal to 0.45 mM and the Hill coefficient = 3.6. The dependence of initial velocities on MgATP concentration is hyperbolic when Fru-6-P is saturating, with a K_m for MgATP

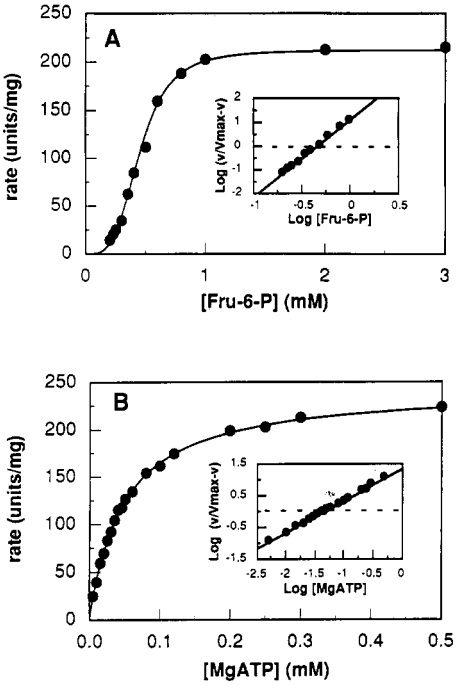

FIGURE 2: (A) Dependence of the rate of the reaction catalyzed by PFK from *E. coli* on Fru-6-P concentration with concentration of MgATP equal to 3 mM. (B) Dependence of the rate on MgATP concentration when Fru-6-P concentration is equal to 4 mM. The inset to each figure shows a corresponding Hill plot.

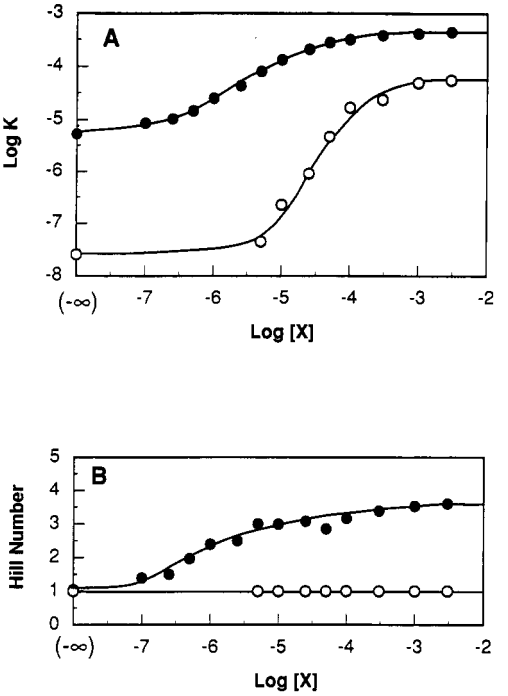

FIGURE 3: (A) Logarithm of the $K_{1/2}$ for Fru-6-P presented as a function of the logarithm of MgATP concentration (●) and logarithm of K_m for MgATP presented as a function of the log of Fru-6-P concentration (○). (B) Hill coefficients determined from the data from which the values of $K_{1/2}$ and K_m presented in panel A were derived.

equal to 49 μM and a Hill coefficient equal to 1 (Figure 2B).

To confirm that the binding monitored with fluorescence in Figure 1 is relevant to the binding of these substrates in a kinetically competent fashion, kinetic assays were performed to determine values of $K_{1/2}$ for Fru-6-P and K_m for MgATP over a broad range of second substrate concentrations. When the concentration of MgATP was decreased from 3 mM to 0.1 μM, the value of $K_{1/2}$ for Fru-6-P decreased from 450 to 8.6 μM (Figure 3A). In the process, Hill numbers also decreased from 3.6 to 1.4 (Figure 3B). As the concentration of MgATP diminishes, both the $K_{1/2}$ and the Hill coefficient approach the values obtained with fluorescence in the absence of MgATP (Figure 1A).

Fru-6-P was similarly varied from 3 mM to 5 μM while the K_m for MgATP was measured. These data are also presented in Figure 3. When Fru-6-P concentration is below $K_{1/2}$ (450 μM), substrate inhibition by MgATP becomes evident, as noted by Kundrot and Evans (1991). As Fru-6-P concentration is further decreased, this MgATP inhibition is manifested at successively lower concentrations of MgATP as shown in Figure 4. However, the substrate inhibition is not due to a typical dead-end mechanism since the curves tend to plateau, rather than diminish to zero, at high MgATP concentrations. Double-reciprocal plots of these data are clearly biphasic, with a clearly defined linear portion at low concentrations of MgATP (data not shown). From the linear portions of these complex double-reciprocal patterns, we estimated a lower limit of the K_m for MgATP to be reduced from 49 μM at 3 mM Fru-6-P to 0.045 μM at 5 μM Fru-6-P (Figure 3A).[2] MgATP binding remains noncooperative in this low concentration regime throughout the entire concentration range of Fru-6-P, as indicated in Figure 3B.

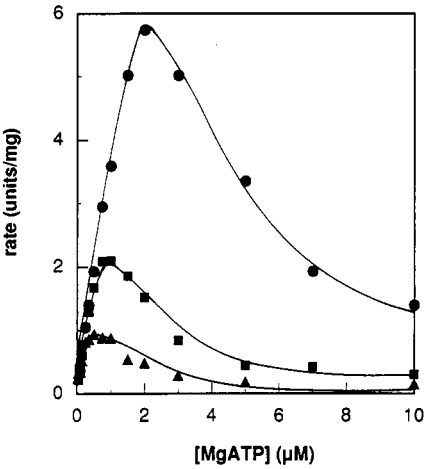

FIGURE 4: Substrate inhibition evident in the saturation profiles for MgATP with Fru-6-P concentration equal to 50 μM (●), 25 μM (■), and 10 μM (▲).

SIMULATION RESULTS

Dimer. The data just presented are characterized by the following distinguishing features: (1) positive cooperativity in the Fru-6-P binding profile when MgATP is saturating; (2) substrate inhibition apparent in the MgATP binding profiles at low concentrations of Fru-6-P; (3) saturable antagonism between Fru-6-P and MgATP. We wish to understand the ligand–ligand coupling interactions that give rise to this behavior. For example, is it necessary to invoke a separate binding interaction, i.e., an allosteric binding for MgATP, as has been proposed previously (Berger & Evans, 1991)?

Clearly, the oligomeric nature of the enzyme must be taken into account in order to fully understand the possible

[2] Nonlinear regression analysis of these data to the functions normally used to describe complete and partial substrate inhibition (Cleland, 1979) failed to converge. Evidently the functional form of the observed inhibition is more complex, which is consistent with our conclusion that this inhibition arises from inter- as well as intrasubunit antagonism in the tetramer (see Discussion).

ramifications of any possible site–site interactions. However, the active form of *E. coli* PFK is a tetramer with four active sites each binding an equivalent of MgATP and Fru-6-P, and a complete linked-function description of such a system is too complex for an explicit solution. We therefore examined the general properties of a dimeric, two-substrate, two-active-site enzyme in an effort to model a mechanism that would at least qualitatively explain the above characteristics.

We derived the rate equation below by modifying the recently published general solution of the rate equation pertaining to a symmetrical dimeric enzyme containing a single substrate and single modifier ligand in rapid equilibrium (Reinhart, 1989) so that both ligands are required for catalytic activity; i.e., both are substrates of a bimolecular reaction. The details of this modification are presented in the appendix below, but the resulting rate equation, assuming maximal velocity of each active site to be the same and invariant, is given by

$$\frac{v}{V_m} = \left[\left(\frac{Q_{aa/bb}Q_{ab2}^2Q_{ab1}^2Q_{bb/a}^2B^2}{Q_{bb}} + Q_{aa/b}Q_{ab2}Q_{ab1}B\right)A^2 + (Q_{ab2}Q_{ab1}Q_{bb/a}B^2 + Q_{ab1}B)A\right] / \left[\left(\frac{Q_{aa/bb}Q_{ab2}^2Q_{ab1}^2Q_{bb/a}^2B^2}{Q_{bb}} + 2Q_{aa/b}Q_{ab2}Q_{ab1}B + Q_{aa}\right)A^2 + 2(Q_{ab2}Q_{ab1}Q_{bb/a}B^2 + [Q_{ab2} + Q_{ab1}]B + 1)A + Q_{bb}B^2 + 2B + 1\right] \quad (2)$$

As applied to the present case, we let $A = [\text{Fru-6-P}]/K_{ia}$ and $B = [\text{MgATP}]/K_{ib}$ where K_{ia} and K_{ib} equal the reciprocals of the thermodynamic binding constants governing the binding of the first equivalent of A and B, respectively. Although the above equation is somewhat complex, it is comprised of parameters that can be intuitively understood and assigned a value on the basis of the experimental data presented in Figures 1–4. Q_{bb} represents the homotropic coupling between the individual bindings of MgATP in the absence of Fru-6-P. Since no cooperativity is evident when MgATP binds, regardless of the concentration of Fru-6-P (Figures 1B and 3B), Q_{bb} must equal 1. Similarly, $Q_{bb/a}$ and $Q_{bb/aa}$, which represent the homotropic coupling between MgATP equivalents when 1 or 2 Fru-6-P equivalents are bound, respectively, must also equal 1. In the same vein, because the binding of Fru-6-P to free enzyme is hyperbolic (Figure 1A), the homotropic coupling between bound Fru-6-P equivalents, Q_{aa}, must also equal 1. Finally, it follows from the values that we have just assigned that the effect of the binding of MgATP on the value of the homotropic coupling for Fru-6-P must be additive; i.e., $Q_{aa/bb} = (Q_{aa/b})^2$, because of linkage identities previously described (Reinhart, 1989; see Appendix). These parameter values allow us to simplify eq 2 to

$$\frac{v}{V_m} = [(Q_{aa/b}^2Q_{ab2}^2Q_{ab1}^2B^2 + Q_{aa/b}Q_{ab2}Q_{ab1}B)A^2 + (Q_{ab2}Q_{ab1}B^2 + Q_{ab1}B)A] / [(Q_{aa/b}^2Q_{ab2}^2Q_{ab1}^2B^2 + 2Q_{aa/b}Q_{ab2}Q_{ab1}B + 1)A^2 + 2(Q_{ab2}Q_{ab1}B^2 + [Q_{ab2} + Q_{ab1}]B + 1)A + B^2 + 2B + 1] \quad (3)$$

Three parameters remain in eq 3 to which values of arbitrary magnitude must be assigned in our simulation. Q_{ab1} reflects the antagonistic coupling between MgATP and Fru-6-P that derives from within a single active site, and Q_{ab2} represents the antagonistic coupling between MgATP and Fru-6-P that would extend between active sites; i.e., the extent to which MgATP binding at site 1 antagonizes the binding of Fru-6-P at site 2. For the purposes of simulation, we assign each of these coupling parameters a value of 0.1, which corresponds to a modest coupling free energy of +1.4 kcal/mol.

From Figure 3 we know that as MgATP binds to the enzyme a positive cooperativity is induced in the binding profile of Fru-6-P. Since the Hill coefficient increases continuously with MgATP saturation and does not diminish when MgATP achieves complete saturation, the coupling parameter that designates the homotropic coupling between Fru-6-P equivalents when MgATP is bound, $Q_{aa/b}$, must have a value greater than 1, which we arbitrarily set equal to 10; i.e., a coupling free energy equal to −1.4 kcal/mol at 25 °C, for the purposes of this simulation.

With these parameter definitions, we can now use eq 3 to describe the binding profiles of A and B at both low and high concentrations of the nonvaried substrate, where concentrations are considered relative to the corresponding dissociation parameter. The results of these simulations are presented in Figure 5.

It is readily apparent that the simulations shown in Figure 5 qualitatively mimic the characteristics evident in Figures 1–4. The saturation curves at low B (MgATP) and high A (Fru-6-P) are both hyperbolic. When B is high, A binds in sigmoidal fashion whereas when A is low the binding of B displays significant substrate inhibition. Moreover, in the absence of A, which can be simulated by letting $Q_{ab1} = Q_{ab2} = 1$, the binding of B is hyperbolic (simulation not shown) as observed for MgATP in the absence of Fru-6-P (Figure 1B). Consequently, we feel that these features can be viewed as deriving from the interconnected relationship between these couplings that are a consequence of the oligomeric features of the enzyme.

Tetramer. Since the equations derived explictly for the dimer by Reinhart (1989) involve the binding of four ligands; i.e., two substrate and two allosteric ligands, the general rate equation for a homotropic tetramer binding four substrate ligands can also be derived by modifying the previous solution as outlined in the appendix. The resulting rate equation is

$$\frac{v}{V_m} = \frac{Q_{aa}^6A^4 + 3Q_{aa}^3A^3 + 3Q_{aa}A^2 + A}{Q_{aa}^6A^4 + 4Q_{aa}^3A^3 + 6Q_{aa}A^2 + 4A + 1} \quad (4)$$

where Q_{aa} represents the average site–site coupling between substrates binding to each of the four active sites. For any given value of Q_{aa} one can calculate from eq 4 the corresponding value of the Hill coefficient. The resulting relationship between Q_{aa} and Hill coefficient is given in Figure 6.

DISCUSSION

There has been some disagreement regarding the kinetic mechanism of *E. coli* PFK. Blangy (1971) concluded that the reaction was ordered with MgATP binding first on the basis of his failure to see with equilibrium dialysis Fru-6-P binding in the absence of ATP. Deville-Bonne et al. (1991b), however, concluded that the order of addition is random because they were able to see Fru-6-P binding in the absence of MgATP via its quenching of intrinsic PFK fluorescence. Dead-end inhibition by analogs of MgATP and Fru-6-P also suggested to Deville-Bonne et al. (1991b) that the substrate addition was random; however, those data are subject to alternative interpretations. Deville-Bonne et al. (1991b) also performed their experiments in the presence of the allosteric activator GDP.

Our data, obtained in the absence of any allosteric effectors, lend further support to the conclusion that Fru-6-P and

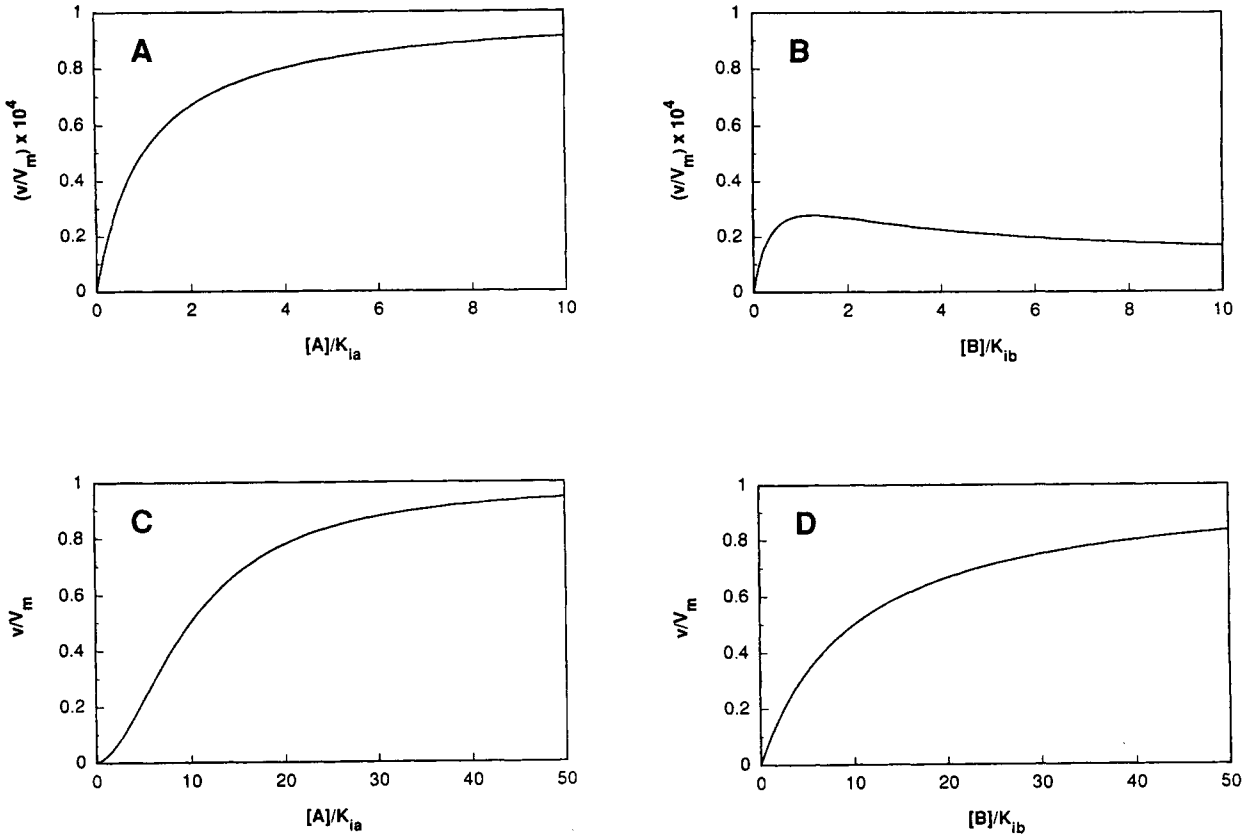

FIGURE 5: Substrate binding behavior predicted by eq 3 for a dimeric, two-substrate enzyme as described in the text assuming an average antagonistic coupling between substrate ligands, Q_{ab}, equal to 0.1 (+1.4 kcal/mol) and an average heterotropically induced homotropic coupling experienced by substrate A when an equivalent of B is bound, $Q_{aa/b}$, equal to 10 (−1.4 kcal/mol). (A) $[B]/K_{ib} = 1 \times 10^{-3}$; (B) $[A]/K_{ia} = 1 \times 10^{-3}$; (C) $[B]/K_{ib} = 1 \times 10^{5}$; (D) $[A]/K_{ia} = 1 \times 10^{5}$. Note in particular the substrate inhibition in panel B and the positive cooperativity in panel C. If one considers substrate A to represent Fru-6-P and substrate B to represent MgATP, panels A–D are qualitatively similar to the behavior exhibited by *E. coli* PFK in figures 1A, 4, 2A, and 2B, respectively.

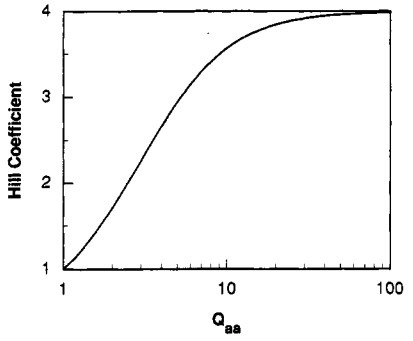

FIGURE 6: Relationship between the average homotropic coupling, Q_{aa}, and the Hill coefficient for a tetramer as predicted by eq 4 described in the text.

MgATP bind in random fashion. Not only have we measured the interaction of both Fru-6-P and MgATP individually with *E. coli* PFK by monitoring their influences on the intrinsic PFK fluorescence, but we have also shown that the same K_d values are approched in kinetic experiments, indicating that the equilibrium binding is kinetically competent. Product inhibition studies of *E. coli* PFK's back-reaction are also consistent with a random mechanism. If the products of the back-reaction (i.e., the substrates of the forward reaction) were released in ordered fashion, the first product to be released would be a noncompetitive inhibitor when either substrate is varied and the nonvaried substrate is subsaturating. Both the Fru-1,6-BP–Fru-6-P and MgADP–MgATP patterns are convincingly competitive, indicating that neither substrate addition nor product release are ordered in the back-reaction. It follows that the same is true in the forward reaction.

There are clearly other features of Fru-6-P and MgATP interactions with *E. coli* PFK that require explanation. MgATP and Fru-6-P antagonize one another's binding substantially, and MgATP induces a positive cooperativity in the Fru-6-P binding profile. It is significant that this latter effect is maximal when MgATP is saturating (Figure 3). The cooperativity Fru-6-P displays is therefore a property of the enzyme–MgATP complex rather than a consequence of Fru-6-P displacing an antagonistic ligand as it binds. Such cooperativity we have previously termed "heterotropically induced homotropic cooperativity" (Reinhart, 1983). The simulations presented in Figure 5 indicate that a two-substrate dimeric enzyme that exhibits heterotropically induced homotropic cooperativity with respect to one substrate and binding antagonism between both substrates will exhibit behavior that qualitatively matches that displayed by *E. coli* PFK: specifically the cooperativity increasingly manifested as MgATP binds and the substrate inhibition by MgATP when Fru-6-P is subsaturating. Consequently, no additional binding interactions, other than the multiple active sites present in the oligomer, are necessary to explain its behavior, contrary to what has previously been suggested (Berger & Evans, 1991). Simulations of other combinations of coupling interactions fail to exhibit comparable behavior (data not shown).

An interesting feature of eq 3 is that a distinction can be drawn between intra-active-site and inter-active-site antagonism between Fru-6-P and MgATP, designated Q_{ab1} and Q_{ab2}, respectively. Simulations in which the antagonism between these substrates is exclusively derived from intra-

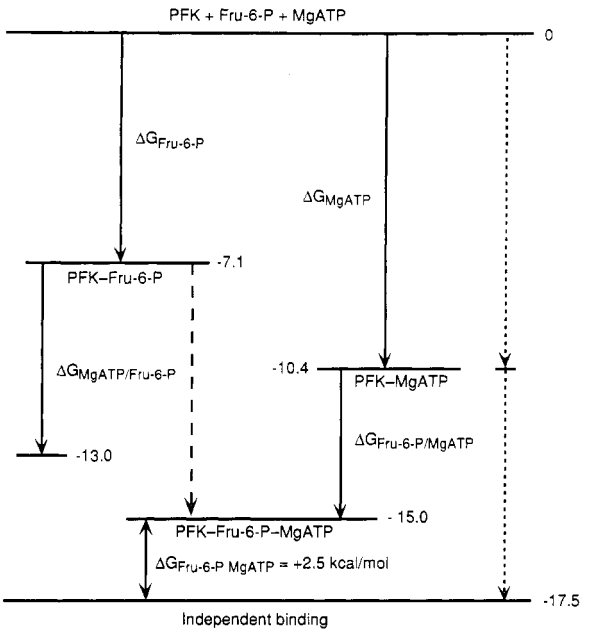

FIGURE 7: Free energy diagram, as developed by Weber (1972, 1975) to demonstrate the reconciliation of the reciprocity requirement for the binding of each substrate with and without the prior binding of the other substrate. The solid arrows labeled ΔG_{MgATP} and $\Delta G_{Fru\text{-}6\text{-}P}$ correspond to the standard free energies calculated from the binding of MgATP and Fru-6-P, respectively, to free enzyme. The total free energy released if the binding of both ligands were independent is obtained from the sum of these two values. The actual free energy realized by the binding of both substrates is obtained by adding the actual free energy release obtained when Fru-6-P or MgATP bind second (i.e., when the other substrate is saturating) and is denoted by $\Delta G_{Fru\text{-}6\text{-}P/MgATP}$ and $\Delta G_{MgATP/Fru\text{-}6\text{-}P}$, respectively. The solid arrow labeled $\Delta G_{MgATP/Fru\text{-}6\text{-}P}$ does not point to the same value as $\Delta G_{Fru\text{-}6\text{-}P/MgATP}$ in apparent violation of the reciprocity requirement for linkage. For the reasons discussed in the text, we believe this is due to the fact that the K_m for MgATP, measured when Fru-6-P is saturating, is not a true thermodynamic quantity. The true value for $\Delta G_{MgATP/Fru\text{-}6\text{-}P}$ would instead correspond to the dashed arrow in the figure. The apparent coupling free energy between Fru-6-P and MgATP, $\Delta G_{Fru\text{-}6\text{-}P\ MgATP}$, is given by the double-headed arrow.

active-site interactions, i.e., $Q_{ab1} < 1$ but $Q_{ab2} = 1$, fail to exhibit substrate inhibition at low values of A, whereas the opposite case, in which the antagonism is entirely inter-active-site, does exhibit substrate inhibition by B at subsaturating A (data not shown). We can conclude, therefore, that the antagonism exhibited by *E. coli* PFK in the binding of Fru-6-P and MgATP is at least partially due to an influence between active sites, contrary to the conclusions of Deville-Bonne et al. (1991b).

One characteristic of our data is not simulated by eq 3, namely, the apparent failure of linkage reciprocity. Thermodynamic linkage dictates that ΔG for the formation of the ternary complex PFK–MgATP–Fru-6-P be the same regardless of the order of substrate addition. However, as shown in Figure 7, our data fail to meet this expectation.

The value of K_d calculated for the interaction of Fru-6-P with *E. coli* PFK in the absence of MgATP is 6.8 μM (Figure 1A), and the K_m for MgATP when Fru-6-P is saturating is equal to 49 μM (Figure 2B), which is equivalent to a free energy change of 7.1 and 5.9 kcal/mol at 25 °C, respectively, if K_m were to represent a thermodynamic value. Consequently, the total free energy of formation of the ternary complex would be −13.0 kcal/mol at 25 °C when Fru-6-P binds first. However, when MgATP is considered to bind first, its K_d is equal to 0.025 μM (Figure 1B) and the $K_{1/2}$ for Fru-6-P after MgATP is bound is equal to 0.45 mM. These values correspond to free energies of 10.4 and 4.6 kcal/mol, respectively, at 25 °C, or a total free energy of formation of the ternary complex of −15.0 kcal/mol. Clearly, in our data the free energy of formation of the ternary complex appears to depend on the order of addition of the two substrates, which violates the fundamental requirement for reciprocity embodied in the principle of thermodynamic linkage (Wyman, 1948, 1964, 1967; Weber, 1972, 1975).

The reason for this discrepancy is not associated with the apparent behavioral asymmetry that results from only one substrate (Fru-6-P) showing cooperative binding behavior in response to the other substrate's binding. The simulations reaffirm that the same apparent coupling parameter describing the influence felt by Fru-6-P to the prior binding of MgATP and vice versa should be obtained in either case. In the case of the simulated dimer, the apparent coupling parameter, Q, should equal the following (Reinhart, 1989):

$$Q = \frac{K^0_{1/2}}{K^\infty_{1/2}} = Q_{ab1}Q_{ab2}Q^{1/2}_{aa/bb} \qquad (5)$$

where the superscripts 0 and ∞ refer to the relative concentration of the substrate to which the $K_{1/2}$ does not pertain. Somewhat surprisingly, this value is obtained regardless of which ligand is considered to bind first despite the fact that the $Q_{aa/bb}$ coupling does not introduce cooperativity in the B binding profiles.

The most reasonable explanation for the apparent failure of linkage reciprocity in our data is that not all of the measured dissociation parameters are equal to thermodynamic values. Of the four values in question, the dissociation constants for Fru-6-P and MgATP in the absence of the other substrate are undoubtedly thermodynamic since they were obtained from thermodynamic as well as kinetic methods. Of the two remaining, we note that MgATP has unusually high affinity in the absence of Fru-6-P and apparently binds an order of magnitude more tightly to form the ternary complex than does Fru-6-P. Consequently, we suspect that MgATP has the highest likelihood of failing to satisfy the rapid-equilibrium condition in the steady state.

Let us for the moment suppose that only MgATP fails to achieve a rapid equilibrium, i.e., that $K_{1/2}$ for Fru-6-P in the presence of saturating MgATP represents the mean of the thermodynamic dissociation constants for Fru-6-P from the ternary complex. Using the values for $K^0_{1/2}$ and $K^\infty_{1/2}$ for Fru-6-P evident in Figure 3A, the true thermodynamic coupling parameter would therefore be equal to

$$Q = \frac{K^0_{1/2}}{K^\infty_{1/2}} = \frac{6.8 \times 10^{-6}\ \text{M}}{4.5 \times 10^{-4}\ \text{M}} = 1.5 \times 10^{-2} \qquad (6)$$

which corresponds to an apparent coupling free energy equal to +2.5 kcal/mol at 25 °C, as denoted by $\Delta G_{Fru\text{-}6\text{-}P/MgATP}$ in Figure 7. Linkage would then dictate that the actual value for the mean thermodynamic MgATP dissociation constant with Fru-6-P bound, K^∞_{ib}, be given by

$$K^\infty_{ib} = \frac{K^0_{ib}}{Q} = \frac{2.5 \times 10^{-8}\ \text{M}}{1.5 \times 10^{-2}} = 1.7 \times 10^{-6}\text{M} \qquad (7)$$

which yields the value for the binding free energy denoted by the dashed arrow in Figure 7.

If we further assume that when Fru-6-P is saturating the enzyme exhibits simple single-substrate behavior with respect to MgATP binding, we can now write the following expression pertaining to the K_m for MgATP when Fru-6-P is saturating:

$$K_m^\infty = \frac{k_{off} + k_{cat}}{k_{on}} = K_{ib}^\infty + \frac{k_{cat}}{k_{on}} = 5 \times 10^{-5}\ M \qquad (8)$$

where the quantity 5×10^{-5} M is obtained from the upper plateau value in Figure 3A. From V_{max}, we know that $k_{cat} = 150\ s^{-1}$, and we can therefore calculate the apparent values of k_{on} and k_{off} to be equal to $3 \times 10^{+6}\ M^{-1}\ s^{-1}$ and $5\ s^{-1}$, respectively. Since k_{off} is substantially smaller than k_{cat}, according to this calculation, MgATP would clearly fail to achieve a binding equilibrium in the steady state. The calculated value of k_{on} is at the lower end, but still within, the range typically found for low molecular weight substrates (Fersht, 1985).

If, as a check of our initial premise, we perform a similar calculation for Fru-6-P, assuming as a reasonable worse case in which k_{on} is equal to that for MgATP, we find that k_{off} is equal to $1.2 \times 10^3\ s^{-1}$, a value 8 times that of k_{cat}. Consequently, we believe that the true value of the coupling between MgATP and Fru-6-P is obtained from the Fru-6-P saturation profiles in the absence and presence of MgATP and that the true value for the thermodynamic dissociation constant of MgATP when Fru-6-P is saturating is given by eq 7 and the thermodynamic coupling is given by eq 6.

As noted above, this apparent coupling (and the corresponding apparent coupling free energy of +2.5 kcal/mol at 25 °C) is composed of contributions from both the antagonistic coupling between Fru-6-P and MgATP, Q_{ab}, and the heterotropically induced homotropic coupling between bound Fru-6-P equivalents when MgATP is saturating, $Q_{aa/bbbb}$. From eq 4, one can derive that in a tetrameric enzyme displaying homotropic cooperativity, $K_{1/2}$ is related to the individual site dissociation constant (i.e., the reciprocal of the binding constant of the first equivalent of A), K_{ia}, by eq 9. (The subscript appended to the Q term and the superscript ∞ designations indicate that the homotropic cooperativity we have observed in Figure 2A is exhibited in the saturating presence of MgATP.)

$$K_{1/2}^\infty = \frac{K_{ia}^\infty}{Q_{aa/bbbb}^{3/2}} \qquad (9)$$

We can now write the following expression that defines the observed coupling parameter Q in terms of the average Fru-6-P–MgATP heterotropic and Fru-6-P–Fru-6-P homotropic interactions:

$$Q = 1.5 \times 10^{-2} = Q_{ab}^4 Q_{aa/bbbb}^{3/2} \qquad (10)$$

where Q_{ab} equals the geometric mean of each individual ATP–Fru-6-P coupling, including the intra-active-site interaction. Note the analogy of eq 10 to eq 5 which pertains to a dimer. $Q_{aa/bbbb}$ can be estimated, from Figure 6 and the limiting Hill coefficient approached at high MgATP concentration in Figure 3B, to be equal to approximately 10 which implies a contribution to the apparent coupling free energy equal to −2.0 kcal/mol at 25 °C. Therefore, the product of all four heterotropic interactions, $(Q_{ab})^4$, is equal to 4.7×10^{-4} (+4.5 kcal/mol total at 25 °C) or each individual MgATP–Fru-6-P coupling is equal to 0.15 (+1.1 kcal/mol at 25 °C) on average. While we do not know how equally the +4.5 kcal/mol coupling free energy is distributed among the 4 MgATP's that can interact with any given Fru-6-P, we can say that some inter-active-site coupling must exist as discussed above.

CONCLUSIONS

Given the ambiguities and difficulties that arise when the responses of PFK to MgATP and Fru-6-P are interpreted with the a priori restriction that only two functionally significant conformations exist, the alternate perspective utilized here would seem to have merit in that it delineates thermodynamic constraints that must be ultimately reconciled by any mechanism. There are four forms of PFK that can be defined unambiguously: free enzyme, enzyme saturated with MgATP, enzyme saturated with Fru-6-P, and enzyme in which both MgATP and Fru-6-P sites are fully occupied. The properties that these four species exhibit with respect to the binding and/or release of MgATP and Fru-6-P can be clearly deduced from the data presented. Free enzyme displays a relatively high affinity for both Fru-6-P and MgATP, with binding constants equal to the reciprocal of 6.8 μM and 25 nM, respectively. These ligands bind to each of their four individual binding sites with little apparent homotropic interaction and hence the same affinity. PFK with Fru-6-P bound in turn binds MgATP with lower affinity than does free enzyme, although MgATP still binds sufficiently tightly that upon binding MgATP has a very high commitment to catalysis. The enzyme–MgATP complex, in contrast, binds the first equivalent of Fru-6-P very weakly. One can estimate the dissociation constant of the first equivalent of Fru-6-P to bind to be equal to $K_{1/2}^\infty(Q_{aa/bbbb})^{3/2}$ = 14 mM (eq 9). However, since Fru-6-P binds to the enzyme–MgATP complex with a positive homotropic interaction (i.e., $\Delta G_{aa/bbbb} < 0$), the affinity for Fru-6-P of the enzyme–MgATP complex increases with Fru-6-P occupancy. Consequently, the ternary complex with both ligands saturating exhibits an affinity for the bound Fru-6-P that is nearly equivalent to that of the free enzyme. The dissociation constant for the first equivalent of Fru-6-P to leave from the 4-fold ternary complex is given by $K_{1/2}^\infty(Q_{aa/bbbb})^{-3/2}$ = 14 μM. On the other hand, MgATP, which does not display positive cooperativity when binding to the enzyme–Fru-6-P complex, remains bound to the ternary complex with comparatively low affinity.

It is clear from this summary that free enzyme, the enzyme–MgATP complex, and the enzyme–Fru-6-P complex all have different attributes with respect to the affinity displayed for both substrates. By this crudest of measures, the enzyme–Fru-6-P complex and the ternary complex exhibit generally similar properties and might reasonably be viewed as representing a single functional class or state. However, given the obvious structural difference between these two species, we suspect that behavioral distinctions with respect to allosteric effectors, pH, etc. will become apparent upon further investigation.

Finally, all of the empirical behaviors of *E. coli* PFK just described can be explained as deriving from two different coupling interactions: Q_{ab} and $Q_{aa/bbbb}$. Q_{ab} represents the average Fru-6-P–MgATP antagonistic interaction, and the corresponding coupling free energy is equal to +1.1 kcal/mol at 25 °C. Simulations convincingly demonstrate that such antagonism, when manifested at least in part between active sites on an oligomeric enzyme, will cause the substrate inhibition evident in the MgATP binding profiles at low Fru-6-P.[3] $Q_{aa/bbbb}$ is the average homotropic coupling between successive Fru-6-P binding interactions when MgATP is saturating, corresponding to a homotropic free energy of interaction equal to −1.4 kcal/mol at 25 °C. This latter coupling parameter is completely independent from the antagonistic heterotropic coupling, and therefore the positive

[3] Indeed, simulations further show that if it were not for the favorable heterotropically induced homotropic coupling Fru-6-P would also exhibit substrate inhibition at low MgATP concentrations (data not shown).

cooperativity experienced by Fru-6-P when MgATP is saturating is not properly viewed as arising from the displacement of a ligand, in this case MgATP, that stabilizes a putative inhibited form of the enzyme.

APPENDIX

Equation 2. The rate equation pertaining to a symmetrical dimeric enzyme with a single substrate, A, and a single allosteric ligand, X, capable of achieving a binding equilibrium in the steady-state to each of the two identical subunits, is given by the following (Reinhart, 1989):

$$v = [(V_a + (V_{ax1}Q_{ax1} + V_{ax2}Q_{ax2})X + V_{axx}Q_{axx}X^2)A + (V_{aa}Q_{aa} + (V_{aax1} + V_{aax2})Q_{aax}X + V_{aaxx}Q_{aaxx}X^2)A^2]/[(1 + 2X + Q_{xx}X^2) + 2(1 + [Q_{ax1} + Q_{ax2}]X + Q_{axx}X^2)A + (Q_{aa} + 2Q_{aax}X + Q_{aaxx}X^2)A^2] \quad (A1)$$

where $A = [A]/K_{ia}$, $X = [X]/K_{ix}$, each V term represents a turnover number, and each Q term represents a coupling parameter. The subscripts indicate the enzyme species, as defined by the bound ligands, to which the parameter pertains. A coupling parameter is equal to a ratio of binding constants in which the numerator consists of the product of the individual binding constants which actually define the equilibria involved in forming the indicated species, and the denominator equals the product of each ligand's binding constant to free enzyme. [See Reinhart (1989) for a detailed discussion.]

Note that there is a term in the numerator that corresponds to each ligated form that can support turnover and each term is multiplied by the turnover number for that enzyme form. The denominator contains a term for each form of the enzyme whether or not substrate is bound. To convert this equation to one that pertains to a two-substrate dimer, the numerator must be modified so that only those enzyme forms to which both ligands are bound simultaneously to the same subunit (i.e., active site) remain. This is easily accomplished by setting V_a, V_{aa}, V_{ax2}, and V_{aax2} to zero. Note that the latter term is equal to 0 because it specifically refers to the turnover of A that is *not* paired with the X that is bound (as distinguished from V_{aax1}). Making these substitutions, as well as changing the notation of the second ligand from X to B to denote its "status" as a substrate, yields the following:

$$v = [(V_{ab1}Q_{ab1}B + V_{abb}Q_{abb}B^2)A + (V_{aab1}Q_{aab}B + V_{aabb}Q_{aabb}B^2)A^2]/[(1 + 2B + Q_{bb}B^2) + 2(1 + (Q_{ab1} + Q_{ab2})B + Q_{abb}B^2)A + (Q_{aa} + 2Q_{aab}B + Q_{aabb}B^2)A^2] \quad (A2)$$

Equation 2 in the text is then obtained by assuming that all of the remaining maximal velocity terms are equal to a common value, designated V_m (i.e., that turnover of the ternary complex at one active site is unaffected by the degree of occupancy of the other active site), as well as substituting the following two-ligand coupling identities to which the multiple coupling parameters appearing in eq A2 are equal (Reinhart, 1989):

$$Q_{aab} = Q_{ab1}Q_{ab2}Q_{aa/b} \quad (A3)$$

$$Q_{abb} = Q_{ab1}Q_{ab2}Q_{bb/a} \quad (A4)$$

$$Q_{aabb} = Q_{ab1}^2Q_{ab2}^2Q_{bb/a}^2\left(\frac{Q_{aa/bb}}{Q_{bb}}\right) \quad (A5)$$

where the subscripts containing a slash indicate a coupling parameter between the ligands indicated to the left of the slash determined while the ligands designated to the right of the slash remain bound.

Equation 3. When deriving eq 3 from eq 2, as described in the text, one must keep in mind the following identity, which corresponds to eq 18 in Reinhart (1989):

$$\frac{Q_{aa}Q_{aa/bb}}{(Q_{aa/b})^2} = \frac{Q_{bb}Q_{bb/aa}}{(Q_{bb/a})^2} \quad (A6)$$

Since all of the terms except $Q_{aa/bb}$ and $Q_{aa/b}$ appearing in A6 are assigned values equal to 1, it follows that $Q_{aa/bb} = (Q_{aa/b})^2$ as stated in the text.

Equation 4. The rate equation pertaining to a single substrate enzyme with four active sites can also be derived from eq A1 by changing all of the second ligands, i.e., X, to the substrate A. If we assume that all of the homotropic interactions are unaffected by the occupancy of the uninvolved sites, then essentially all of the two ligand couplings become equal. Note that it is from the identities A3 through A5 that the powers to which the homotropic couplings are raised in eq 4 originate. Equation 4 in the text was derived by making these substitutions as well as by assuming the equivalency of each turnover coefficient.

REFERENCES

Berger, S. A., & Evans, P. R. (1991) *Biochemistry 30*, 8477–8480.

Blangy, D. (1971) *Biochimie 53*, 135–149.

Blangy, D., Buc, H., & Monod, J. (1968) *J. Mol. Biol. 31*, 13–35.

Bradford, M. (1976) *Anal. Biochem. 72*, 248–254.

Cleland, W. W. (1963) *Biochim. Biophys. Acta 67*, 104–137.

Cleland, W. W. (1967) *Adv. Enzymol. Relat. Areas Mol. Biol. 29*, 1–32.

Cleland, W. W. (1979) *Methods Enzymol. 63*, 500–513.

Deville-Bonne, D., Bourgain, F., & Garel, J.-R. (1991a) *Biochemistry 30*, 5750–5754.

Deville-Bonne, D., Laine, R., & Garel, J.-R. (1991b) *FEBS Lett. 290*, 173–176.

Fersht, A. R. (1985) in *Enzyme Structure and Mechanism*, pp 150–151, Freeman, New York.

Hill, A. V. (1910) *J. Physiol. London 40*, iv–vii.

Kotlarz, D., & Buc, H. (1982) *Methods Enzymol. 90*, 60–70.

Kundrot, E. E., & Evans, P. R. (1991) *Biochemistry 30*, 1478–1484.

Monod, J., Wyman, J., & Changeux, J. P. (1965) *J. Mol. Biol. 3*, 318–356.

Reinhart, G. D. (1983) *Arch. Biochem. Biophys. 224*, 389–401.

Reinhart, G. D. (1989) *Biophys. Chem. 30*, 159–172.

Rubin, M. M., & Changeux, J.-P. (1966) *J. Mol. Biol. 21*, 265–274.

Smith, D. K., Krohn, R. I., Hermanson, G. T., Mallia, A. K., Gartner, F. H., Provenzano, M. D., Fujimoto, E. K., Goeke, N. M., Olson, B. J., & Klenk, B. C. (1985) *Anal. Biochem. 150*, 76–85.

Weber, G. (1972) *Biochemistry 11*, 864–878.

Weber, G. (1975) *Adv. Protein Chem. 29*, 1–83.

Wyman, J. (1948) *Adv. Protein Chem. 4*, 407–531.

Wyman, J. (1964) *Adv. Prot. Chem. 19*, 223–286.

Wyman, J. (1967) *J. Am. Chem. Soc. 89*, 2202–2218.

Zheng, R.-L., & Kemp, R. G. (1992) *FASEB J. 6*, A335.